

Preparation of High-Strength and High-Modulus Poly(Vinyl Alcohol) Fibers by Crosslinking Wet Spinning/Multistep Drawing Method

KUEN-SHAN HWANG,* CHIN-AN LIN, and CHUNG-HUA LIN

Graduate Institute of Textile Engineering, Feng Chia University, Taichung, Taiwan, Republic of China

SYNOPSIS

This study is mainly focused on the preparation of high-strength and high-modulus poly(vinyl alcohol) (PVA) fibers by crosslinking wet spinning and multistep drawing. High strength as well as high modulus can be achieved by introduction of the crosslinks into the oriented chains to reduce entanglement degree and slippage between chains. The relationships between mechanical properties and fine structure of the drawn fibers were examined based on results of measurements of tensile property, thermal property, dynamic viscoelasticity, crystallinity, and orientation. The strength and Young's modulus of the drawn fibers are approximated to 1.82 and 51.76 GPa, respectively. The fiber has a sharp melting peak temperature that appeared at 236.7°C in the differential scanning calorimeter (DSC) curve. Our results indicate the multistep drawing procedure is superior to the conventional one-step drawing procedure. These excellent mechanical properties can be directly attributed to their high orientation of the amorphous chains. © 1994 John Wiley & Sons, Inc.

INTRODUCTION

Recently, preparation of high-strength and high-modulus polymer materials have been actively pursued with considerable interest in the relationships between mechanical properties and fine structure. Many different processing approaches have been reported: high-speed melt spinning,¹ gel state spinning,^{2,3} zone drawing,⁴ crystallization in flowing solution,⁵ high-pressure extrusion,^{6,7} hot drawing,⁸ superdrawing,⁹ and so on. The crosslinking wet spinning technique first appeared in the patent literature in late 1960s and early 1970s.¹⁰⁻¹³ However, only in recent years, it has started to attract increasing commercial interest.¹⁴⁻¹⁸

On the other hand, poly(vinyl alcohol) (PVA) has a very high potential for preparation of high-strength and high-modulus fibers because of its superior qualities of impact strength, crystalline modulus, weather durability, antialkaline resistance, and

so on.¹⁹ However, nothing has been reported about the properties of high-strength and high-modulus PVA fibers after multistep drawing. We have intended to produce high-strength and high-modulus PVA fibers by an innovative "crosslinking wet spinning/multistep drawing" processing technique.

The object of the present study is to examine experimentally the fine structure arrangement and to obtain a fully extended chain crystal. It is found that the obtained fiber has excellent mechanical properties in spite of the sample procedure used.

EXPERIMENTAL

Material

The raw material PVA from Chang Chun Petrochemical Co. Ltd. has a polymerization degree of 1700 and a saponification value of 99.6%. The concentration of PVA and boric acid in the spinning process were varied from 10 to 20% and 0 to 3%, respectively. Spinning speed was set at 5.4 m/min. The fibers were spun through nozzles with diameters ranging from 0.2 to 0.8 mm, and at a 60°C coagu-

* To whom correspondence should be addressed.

lation bath. A modified wet spinning machine was used in this study.

Drawing Procedure

The drawing procedure used to produce high-strength and high-modulus PVA fibers was the multistep drawing process. It was applied to arrange the molecular chains of the PVA material. All of the multistep drawing was performed with a hot oven between two rollers. Draw ratios were controlled by selection of back roller speeds. Special clamps were designed to prevent slippage and gripping of the fibers during drawing stages. Each stage draw ratio for all fibers was 10 m/min, which corresponds to a draw ratio of 1.5 times for a gauge length of 100 cm. The high draw ratio was attained when the drawing just before melting temperature was repeated several times. Drawing temperature was controlled to within 2°C by a control system. Mechanical and physical properties of the fibers were determined at least 24 h after drawing. In this study, one-step drawing and multistep drawing processes were abbreviated as 1SD and MSD, respectively.

Tensile Test

Ultimate strength, elongation, and Young's modulus of each fiber were measured in an Instron tensile tester model 1122. Gauge length was set to 20 mm. Crosshead speed was 100 mm/min. Each ultimate strength and elongation value reported here represents an average of 10 individual measurements.

Wide-Angle X-ray Diffraction (WAXD)

Crystalline size along the fiber axis was estimated using wide-angle X-ray diffraction (WAXD) with a Rigaku X-ray diffractometer. The integral breadth of the chain direction (020) reflection (PVA has a monoclinic crystal structure) was used in the Scherrer equation²⁰

$$L = \frac{k\lambda}{\beta \cos \theta} \quad (1)$$

where k is a constant (generally equal to 0.9), L represents the average size of crystalline perpendicular to the planes, β is the width at half maximum intensity of the pure reflection profile in radian, λ is the X-ray wavelength, and θ is the Bragg angle. The pure reflection profile for planes was obtained from the resolution of the diffraction from $2\theta = 60^\circ$

to $2\theta = 5^\circ$, corresponding to the major peak in the equatorial direction.

The crystalline orientation function was calculated from the angular width of the (101) equatorial reflection using the Hermans equation²¹

$$f_c = \frac{3\langle \cos^2 \phi \rangle - 1}{2} \quad (2)$$

where f_c is the crystalline orientation factor, ϕ is the angle between the fiber axis and the molecular chain axis, and the average denoted by the angle brackets is determined as follows:

$$\langle \cos^2 \phi \rangle = \frac{\int_0^{\pi/2} I(\phi) \cos^2 \phi \sin \phi \, d\phi}{\int_0^{\pi/2} I(\phi) \sin \phi \, d\phi} \quad (3)$$

where $I(\phi)$ is the X-ray intensity of the resolved peak at the azimuthal angle ϕ . In this case, the planes of (100) and (001) observed at Bragg angle of 10.5° and 15.5° , respectively.

The amorphous orientation factor was evaluated by combining X-ray and optical birefringence data.²¹ Birefringence was measured using a Zeiss polarizing microscope. Amorphous orientation factors were then calculated by the following equation:

$$\Delta n = x_c \Delta n_c^0 f_c + (1 - x_c) \Delta n_a^0 f_{am} + \Delta n_f \quad (4)$$

where Δn is the measured birefringence, Δn_c^0 and Δn_a^0 are the intrinsic birefringence of the crystalline and amorphous phase, X_c is the degree of crystallinity of the fibers, and f_c and f_{am} are the crystalline and amorphous orientation factor of the fibers, respectively. The form birefringence Δn_f is neglected. The value of $\Delta n_c^0 = 51.8 \times 10^{-3}$ and $\Delta n_a^0 = 43.8 \times 10^{-3}$ were used.²²

Dynamic Mechanical Analysis

The storage modulus E' and the loss modulus E'' of the as-spun fibers and drawn fibers were measured by a Rheovibron DDV-II-C dynamic viscoelastometer. This instrument measures the temperature dependence of the complex modulus E^* and $\tan \delta$ of a viscoelastic solid at a particular frequency. The testing was done over a temperature range of 25–240°C, at a heating rate of 3°C/min, and at a frequency of 3.5 Hz. It is noted that nitrogen was applied to the testing chamber to prevent the speci-

Table I Most Suitable Conditions for Multistep Drawing

Conditions	MSD							
	1SD	(1)	(2)	(3)	(4)	(5)	(6)	(7)
Temp. of drawing (°C)	220				220			
Repetition (times)	1	1	1	1	1	1	1	1
Total draw ratio	15.6	6.1	7.3	10.5	12.6	15.2	18.2	21.9

mens from absorbing water. According to the linear viscoelasticity theory,²³ it can be shown that

$$E^* = E' + iE'' \quad (5)$$

where E' is the storage modulus, and E'' is the loss modulus. The relationship between E' and E'' is given by:

$$\tan \delta = E''/E' \quad (6)$$

Differential Scanning Calorimeter (DSC)

Thermal analyses were performed on a DuPont 910S differential scanning calorimeter. Approximate 7 mg of the fibers were taken together for each run. DSC curves were obtained in the temperature range of 25–300°C and at a scanning rate of 10°C/min. The melting points of the fibers were taken as the position of the maximum of the melting curves.

Scanning Electron Microscope (SEM)

The microfibrillar structure of fibers prepared by peel back was observed using a Bausch & Lomb Ltd. Nanolab 2100 scanning electron microscope (SEM) at 15 kV after the specimen had been coated with a gold layer.

RESULTS AND DISCUSSION

The purpose of multistep drawing is to obtain a highly oriented fiber. The lower draw ratio of every

one-step drawing would make a higher draw ratio. The as-spun fibers contained lamellae structure,¹⁸ to more effectively unfold the lamellae, it was necessary to repeat the hot drawing. As shown in Table I, the multistep drawing was repeated 7 times and the draw ratio in each stage was 1.5 times. We used multistep drawing PVA fibers to obtain a higher draw ratio and better physical properties. Table II shows the strength, elongation, and Young's modulus of the fibers prepared by the one-step and multistep drawing procedure. It was found that the tensile properties of the fibers prepared by the multistep procedure were definitely superior to those by the one-step procedure. Figure 1 shows the stress-strain curves of as-spun, one-step drawing, and multi-step drawing PVA fibers at 220°C. It can be seen that the drawing process plays an important role in improving the mechanical properties of PVA fibers.

The strength, elongation, and Young's modulus of multistep drawing fibers were obtained from the stress-strain curves, showing that the strength of fibers is increased with the draw ratio. It is because as the fibers were extended, the inner molecular chains would become more oriented to the fiber axis. The strength increased in consequence; the elongation would decrease because of the increase of draw ratio because extension would cause the molecular chains to become more orderly. Figure 2 shows the relationship between draw ratio and Young's modulus of multistep drawing PVA fibers. As illustrated in this figure we found a linear relationship between Young's modulus and draw ratio. The Young's modulus rapidly increased by multistep drawing procedures. The maximum value of Young's

Table II Tensile Properties of As-Spun Fibers, One-Step Drawing Fibers and Multistep Drawing Fibers

Sample	High Possible Draw Ratio	Strength (GPa)	Elongation (%)	Young's Modulus (GPa)
As-spun	—	0.18	62.5	4.67
1SD	15.6	1.39	18.1	32.35
MSD	21.9	1.82	7.4	51.76

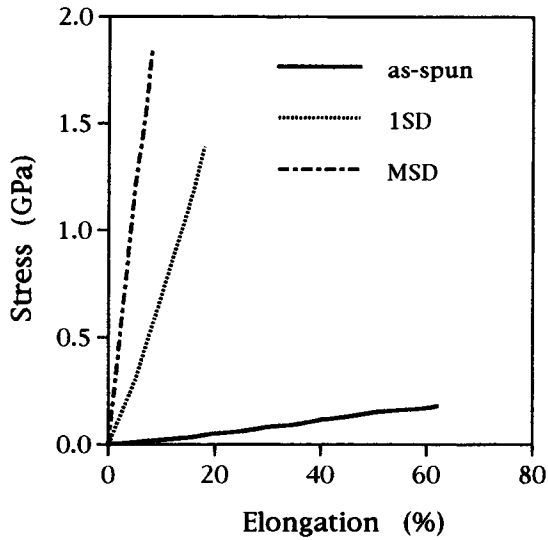


Figure 1 Stress-strain curves for three kinds of PVA fibers: (a) as-spun, (b) one-step drawing, (c) multistep drawing.

modulus, 51.76 GPa, was 1.6 times that of one-step drawing fibers, 32.35 GPa.

X-ray diffraction data were used to determine the crystalline size from Eq. (1), and the results are shown in Figure 3. No significant change was detected in crystalline size of various fibers during the fiber spinning procedure. But more extended drawing at high temperature occurred just before the PVA melting point, presumably a consequence of a further increase in crystalline perfection and size. From an

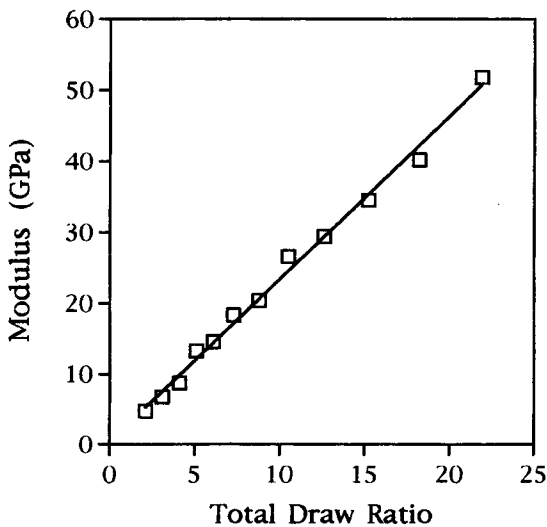


Figure 2 Relationships between the total draw ratio and Young's modulus for multistep drawing fibers.

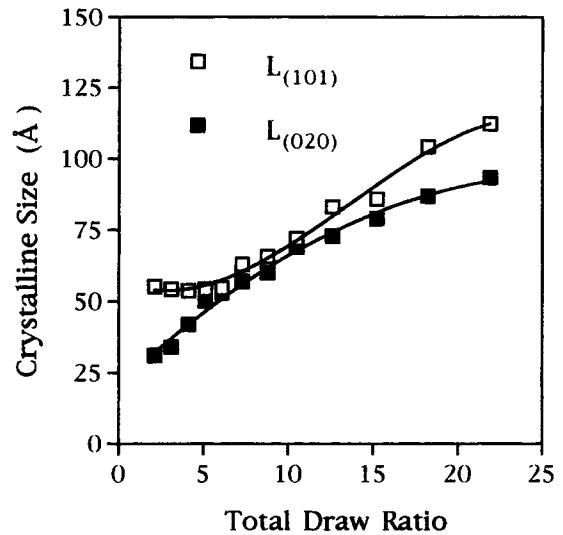


Figure 3 Total draw ratio dependence of the crystalline size for multistep drawing fibers.

initial value of 55 Å, crystalline size increased to about 112 Å at high draw ratios. The crystalline size increased in the range of draw ratio considered here. The crystalline size of the various PVA fibers were apparently different. The multistep drawing seemed to impose greater changes on crystalline size than one-step drawing.

Figure 4 shows the relationship between draw ratio and crystallinity. It is found that the crystallinity was increased with draw ratio because of the effect of extension disordered the lamellae, which made

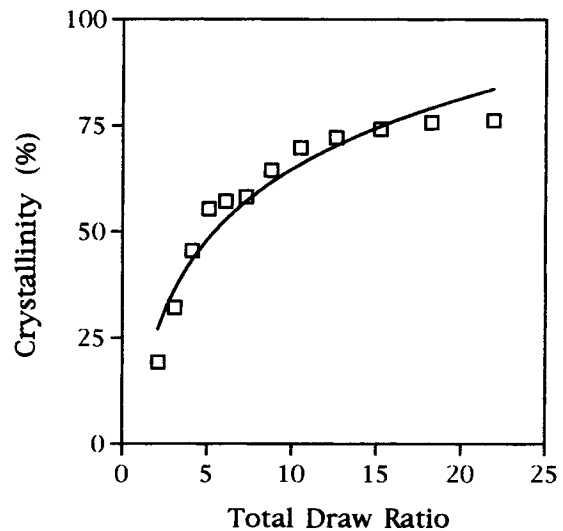


Figure 4 Crystallinity versus total draw ratio for multistep drawing fibers.

the folding chain slant as well as glide, and then ordered them parallel. As the draw ratio increased, the orientation of molecular chains would increase as well, and it would be easy for them to arrange themselves tightly and firmly.

The amorphous orientation factor was calculated with the help of Eq. (4) from measured crystallinity, crystalline orientation, and birefringence and using the values of intrinsic birefringence as obtained elsewhere. Figure 5 presents the draw ratio dependence of the crystalline orientation factors and amorphous orientation factors of multistep drawing fibers. It showed that the crystalline orientation is increased with of the fibers followed the increased of draw ratio. When the draw ratio is increased, the molecular chains are then pulled straight and then make the arrangement of chains become more parallel to the fiber axis. In this case, the crystalline orientation is increased as the draw ratio increased. This is shown in Figure 5. As shown in Figure 6, the birefringence would increase with the draw ratio. These results illustrated that while the molecular chains between crystalline and amorphous regions were extended, they would become more parallel to the fiber axis.

The dynamic loss tangent which is the ratio between the loss and storage modulus is shown in Eq. (6). This ratio could be also interpreted as the fraction of energy lost per cycle due to viscous dissipation caused by friction of molecules during chain segment motion. Therefore any restrictions to segment mobility, and thereby reduction of chain slip-

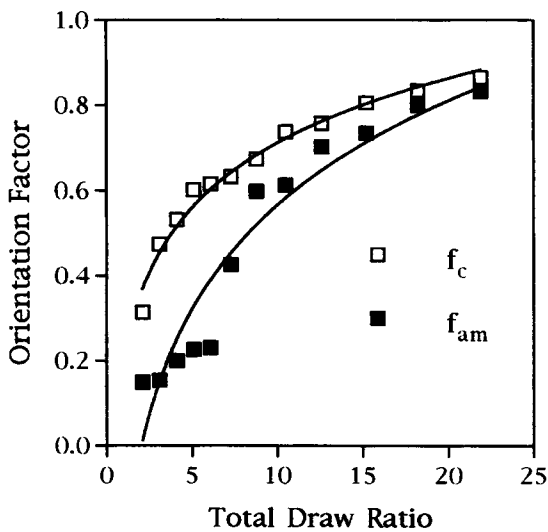


Figure 5 Relationships between the total draw ratio and orientation factor for multistep drawing fibers.

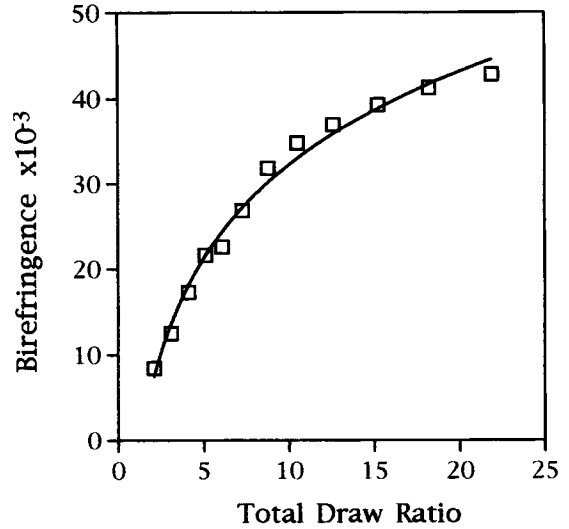


Figure 6 Dependence of the birefringence on the total draw ratio.

page, should reduce the magnitude of δ or require higher energy to effect the motion. Figures 7 and 8 show the temperature dependence of the dynamic storage modulus E' and loss tangent $\tan \delta$, respectively. The value of E' increased with draw ratio over the range of temperature. The reduction of E' above the primary relaxation temperature became less distinct for higher draw ratio samples. In the fiber structure displaying the small reduction of E' , the fraction of tie molecules seemed to be increased as the amorphous regions were included in the crys-

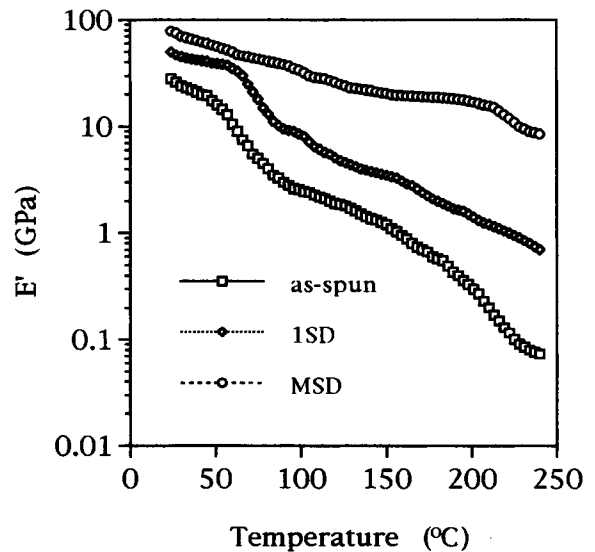


Figure 7 Temperature dependence of the dynamic storage modulus E' for three kinds of PVA fibers.

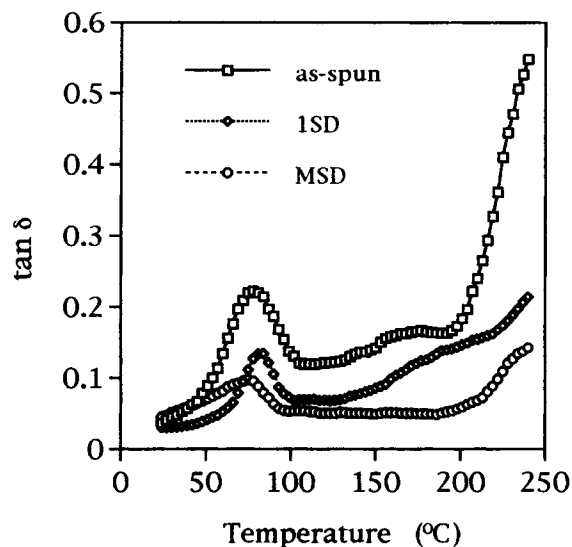


Figure 8 Temperature dependence of the loss tangent, $\tan \delta$, for three kinds of PVA fibers.

talline segment. The E' value was still low for the one-step drawing but was rapidly increased for the multistep drawing over all the temperature ranges. The $\tan \delta$ peak located around 80°C corresponding to the primary relaxation was associated with the initiation of the microbrownian motion of amorphous chains. The maximum value of $\tan \delta$ was related to the volume fraction of the amorphous region, while the temperature of the maximum $\tan \delta$ was related to the molecular packing density of the amorphous regions. A peak broadening could then

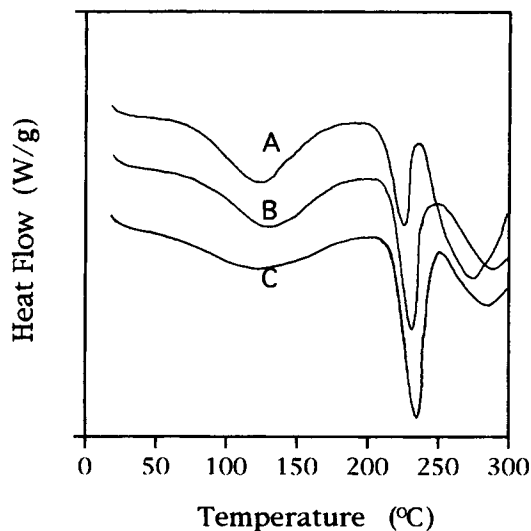


Figure 9 DSC heating curves of PVA fibers. Scanning speed $10^\circ\text{C}/\text{min}$: (a) as-spun, (b) one-step drawing, (c) multi-step drawing.

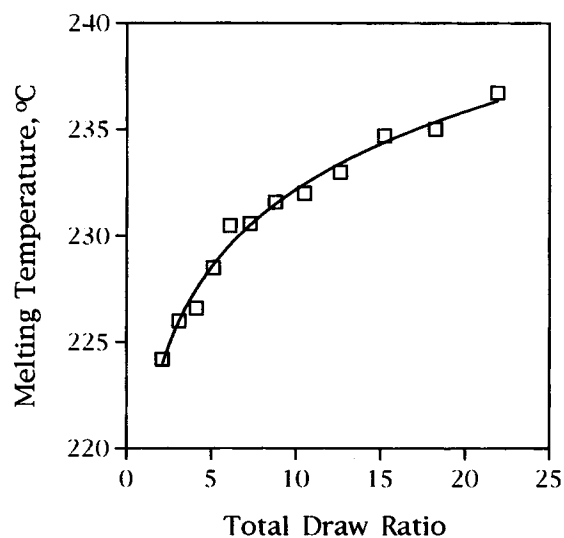


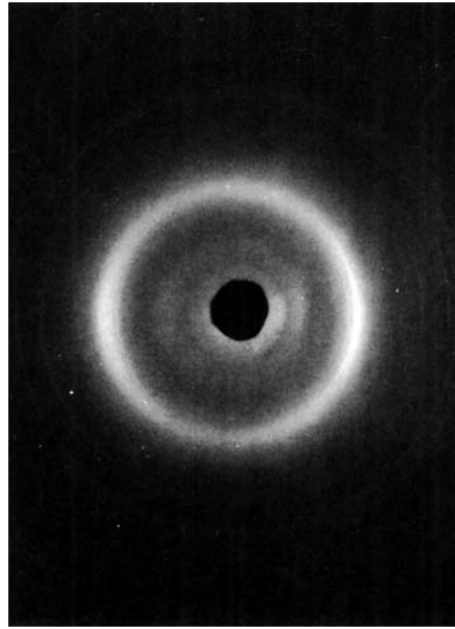
Figure 10 DSC melting temperature versus total draw ratio of PVA fibers.

be interpreted as the consequence of the distribution of molecular packing density in amorphous regions. The decrease of $\tan \delta$ at all draw ratios could then be explained by increase of the crystallinity and birefringence, as shown in Figures 4 and 6. It can be considered that the multistep drawing fibers contain numerous high-quality crystallinity. This can be shown from the results of DSC measurement. The melting peak become steeper and shifted to higher temperature.

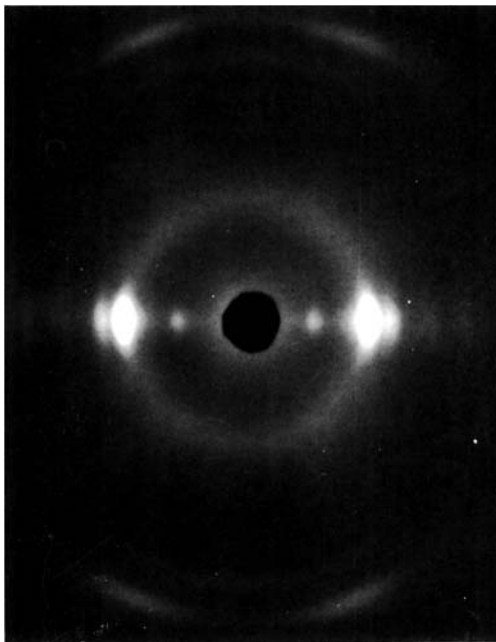
This section dealt in brief with the thermal properties of the PVA fibers, which were studied by DSC. It should be noted that a standard heating rate of $10^\circ\text{C}/\text{min}$ was adopted in this experiment. In Figure 9 DSC heating curves are shown the as-spun fiber, one-step drawing fiber, and multistep drawing fiber. Similar to the mechanical properties, the thermal properties were found to depend strongly on the draw ratio. The as-spun fiber had a peak melting temperature of 224.2°C and one-step drawing fiber of 232.6°C . The peak melting temperature of mul-

Table III Crystallinity (X_c), Orientation Factors of Crystalline and Amorphous (f_c and f_{am}), and Birefringence (Δn) of As-spun Fibers, One-Step Drawing Fibers, Multistep Drawing

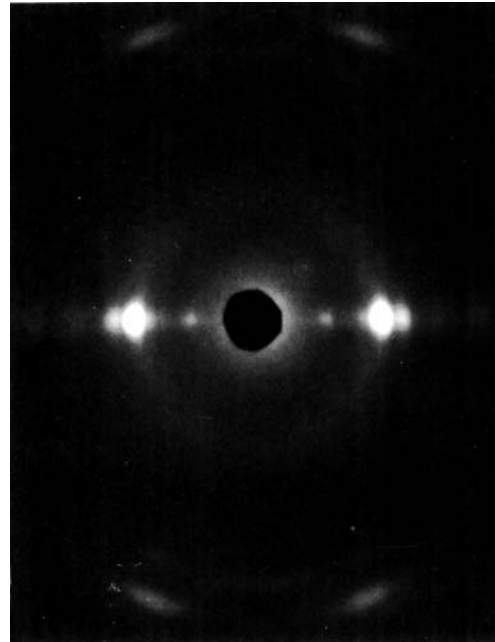
Sample	X_c (%)	f_c	f_{am}	$\Delta n \times 10^3$
As-spun	19.4	0.313	0.149	8.42
1SD	74.0	0.805	0.785	39.80
MSD	76.2	0.865	0.832	42.82



as-spun



one-step drawing

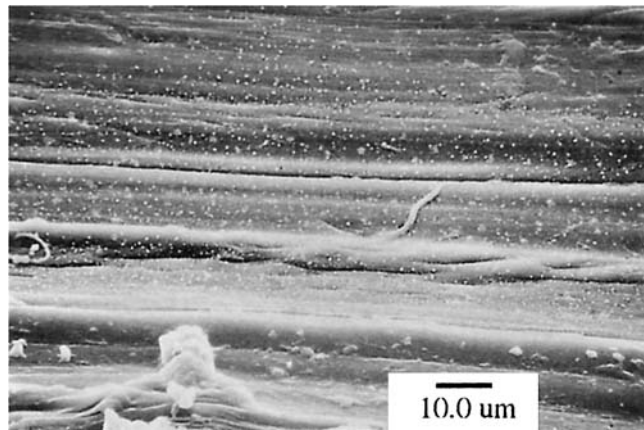


multi-step drawing

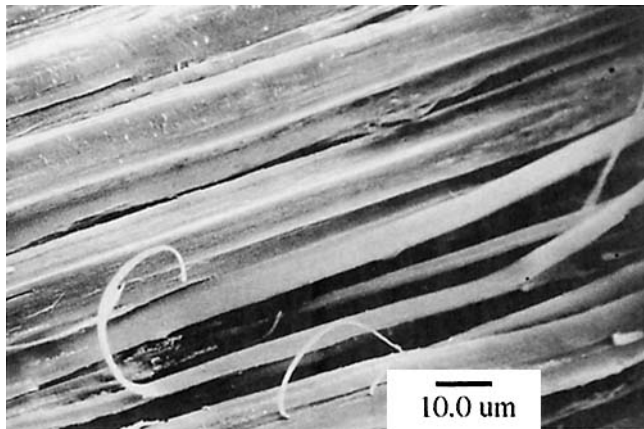
Figure 11 WAXD photographs for three kinds of PVA fibers.

tistep drawing PVA fibers are shown in Figure 10. The melting point rapidly increased with draw ratio, reaching a value of 236.7°C at a draw ratio of 21.9. This value is higher than the one-step drawing fiber samples. Comparison of the melting points is shown

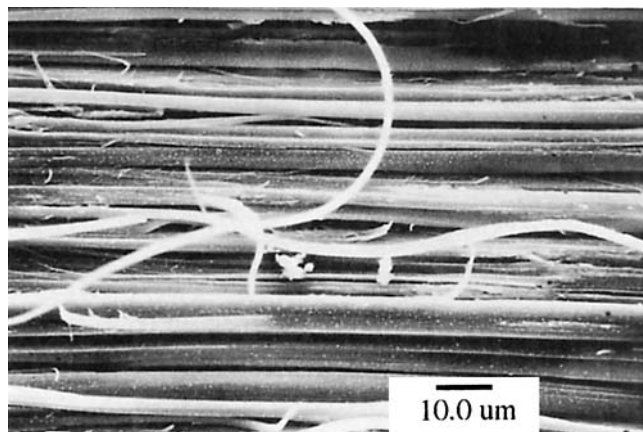
in Figure 10. We think that, the crystallinities prevent the movement and relaxation of the amorphous chains and contribute directly to maintenance of the high modulus. The heat of fusion of the fibers showed a similar dependence on the draw ratio as



as-spun



one-step drawing



multi-step drawing

Figure 12 SEM micrographs of PVA fibers prepared by peelback method to reveal the internal fibrillar structure.

the melting temperature. The values of the as-spun fiber and one-step drawing fiber were 29.6 and 110.1 J/g, respectively. The heat of fusion of the multistep drawing fibers rapidly increased with the draw ratio, reaching a value of 116.4 J/g at a draw ratio of 21.9. This corresponds to an increase in crystallinity from 19.4 to 76.2% if based on a value of 156.2 J/g for fully crystalline PVA.

Table III shows the crystallinity, orientation factors of crystalline and amorphous regions, and birefringence for different draw ratio of fibers. The values of all the orientation factors were arranged in the same order as in the case of the mechanical properties. This tendency also can be clearly seen in X-ray photographs, as shown in Figure 11, in which each crystal plane reflection became narrow from arc to spot in the same order. Closer examination of Table III shows that, although the f_c values were fairly high, values for all the fibers and arc were roughly in the same order. In contrast to f_c and X_c , f_{am} is increased with the processing and was proportional to the Young's modulus and dynamic storage modulus E' . This suggests that the orientation, especially the orientation of amorphous molecular chains, plays an important role in the development of the mechanical properties. The birefringence value of the multistep drawing fibers reached 42.82×10^{-3} , a value quite close to the intrinsic birefringence values, which had been previously reported.²² On the other hand, the magnitude of the crystallinity was not directly related to the mechanical properties.

Structural morphology study can be conducted by simple peeling methods for scanning electron microscope (SEM). PVA fibers peeled back to reveal their internal structure show the microfibrillar structure, as shown in Figure 12. It shows the splitting of the multistep drawing fibers after peeling with a number of fibrils parallel to the fiber axis, so that the drawn fiber has a microfibrillar structure associated with high orientation.

We gracefully thank Dr. C. C. Bai of the Industrial Technology Research Institute and Prof. T. W. Shyr of Textile Engineering of Feng Chia University for their valuable opinion and support. Special thanks are also extended to

the Chang Chun Petrochemical Co. Ltd. for their generous offer of material.

REFERENCES

1. S. L. Kwolek, U.S. Pat. 3,671,542 (1972).
2. P. Smith and P. J. Lemstra, *J. Mater. Sci.*, **15**, 505 (1980).
3. B. Kalb and A. J. Pennings, *J. Mater. Sci.*, **15**, 2584 (1980).
4. T. Kunugi, T. Kawasumi, and T. Ito, *J. Appl. Polym. Sci.*, **40**, 2101 (1990).
5. A. J. Mchugh, P. Vaughn, and E. Ejike, *Polym. Eng. Sci.*, **18**, 443 (1978).
6. N. E. Weeks and R. S. Porter, *J. Polym. Sci., Polym. Phys. Ed.*, **12**, 635 (1974).
7. A. G. Gibson and I. M. Ward, *J. Polym. Sci., Polym. Phys. Ed.*, **16**, 2015 (1978).
8. W. Wu and W. B. Black, *Polym. Eng. Sci.*, **19**, 1163 (1979).
9. K. Yamaura, T. Tanigami, N. Hayashi, K-I Kosuda, S. Okuda, Y. Takemura, M. Itoh, and S. Matsuzawa, *J. Appl. Polym. Sci.*, **40**, 905 (1990).
10. T. Ashikaga, U.S. Pat. 3,660,556 (1969).
11. Kuraray Co., Jpn. Pat. 46-11457 (1971).
12. Unitika Co., Jpn. Pat. 46-28220 (1971).
13. Kuraray Co., Jpn. Pat. 47-50337 (1972).
14. Kuraray Co., Jpn. Pat. 62-104912 (1987).
15. Unitika Co., Jpn. Pat. 62-149909 (1987).
16. H. Fujiwara, M. Shibayama, J-H Chen, and S. Nomura, *J. Appl. Polym. Sci.*, **37**, 1403 (1989).
17. M. Shibyama, T., Hayasaki, J-H Chen, S. Nomura, and H. Fujiwara, *Sen-i Gakkaishi*, **46**(1), 15 (1990).
18. T. Hayasaki, M. Shibayama, S. Sakurai, S. Nomura, H. Fujiwara, and S. Suehiro, *Sen-i Gakkaishi*, **47**(1), 5 (1991).
19. I. Sakurada, *Polyvinyl Alcohol Fibers*, Marcel Dekker, New York, 1985.
20. L. E. Alexander, *X-ray Diffraction Method in Polymer Science*, Wiley, New York, 1969.
21. R. J. Samuels, *Structured Polymer Properties*, Wiley, New York, 1974.
22. S. Hibi, M. Maeda, and M. Takeuchi, *Sen-i Gakkaishi*, **27**(2), 41 (1971).
23. J. D. Ferry, *Viscoelastic Properties of Polymer*, 2nd ed., Wiley, New York, 1970.

Received July 14, 1993

Accepted November 22, 1993